Scaling laws for atomic and molecular hydrogen in a multicusp ion source

J. H. M. Bonnie, P. J. Eenshuistra, and H. J. Hopman
Association EURATOM-FOM, FOM-Instituut voor Atoom-en Molecuulfysica, Kruislaan 407, NL-1098 SJ Amsterdam, The Netherlands
(Received 20 July 1987)

We have determined scaling laws for the densities of atomic and molecular hydrogen in a discharge. For diagnosis we use a multiphoton-ionization technique. Both atoms and molecules are detected in their electronic ground state. The lowest three vibrational levels of the molecules, with vibrational quantum numbers $v''=0$, 1, and 2, are investigated separately. From the scaling laws for the $v''=1$ and 2 populations, we obtain experimental evidence that they are produced by low-energy-electron collisions with unexcited molecules, and are destroyed predominantly by collisions with other discharge-produced particles, presumably atoms and/or thermal electrons. Scaling laws concerning the atomic density are found to be compatible with production mainly via primary electron excitations of electronic ground-state molecules and destruction dominated by wall collisions.

I. INTRODUCTION

During recent years considerable effort has been put into the generation of intense beams of negative ions, extracted from so-called "volume sources," containing magnetically confined hydrogen plasmas.[1] Despite the impressive progress in this field and the work that has been done on the fundamental processes occurring in these devices, both theoretically and experimentally,[2-10] opinions still differ as to the explanation for the abundance of negative ions. However, the presumption has found wide acceptance that these ions are produced through dissociative electron attachment (DA) to rovibrationally excited electronic ground-state molecules,[4] generally designated by the symbol $X\,^1\Sigma_g^+(v'',J'')$, with v'' and J'' the vibrational and rotational quantum numbers, respectively. The dependence of the cross section for this reaction on v'' and J'' has been investigated experimentally[11] (up to $v''=4$), as well as theoretically.[12] Due to the strong increase of the cross section with v'', molecules with $v''\geq 5$ are the chief contributors to the total H^- density.[5,6] The dominant processes which are believed to lead to vibrationally excited molecules in hydrogen discharges have been discussed by several authors.[5,6] Low-energy electrons populate the lower vibrational levels ($v''\leq 4$) through a resonant mechanism involving the temporary formation of H_2^- which is called the e-V process. On the other hand, in the E-V process high-energy electrons excite the molecules to singlet electronically excited states followed by radiative decay back to the electronic ground state with $v''>0$. Depending on the discharge parameters, either the E-V process or Auger neutralization of H_2^+ ions impinging on the chamber wall is believed to be the main source of molecules with $v''\geq 5$.[6] Vibrationally excited molecules may be destroyed by several mechanisms like V-T processes (in which vibrational energy is converted into translational energy during molecule-molecule collisions), electron ionization (e-I) or electron dissociation (e-D) processes, wall deexcitation processes or vibrational deexcitation via atom-exchange collisions.[5,6] Not only the DA process, but also the vibrational excitation and deexcitation processes have cross sections for which the dependences on the initial quantum state of the molecules involved are often unknown or at least incomplete.[5]

In order to test the assumptions made in and results deduced from models describing the plasma chemistry of volume sources, the vibrational distribution of the hydrogen molecules in such a discharge must be measured. For this purpose Pealat *et al.*[8] measured this distribution up to $v''=3$ using coherent anti-Stokes Raman spectroscopy (CARS). Owing to a lack of sensitivity they were unable to detect the higher vibrational levels. Therefore we have set up an experiment[13] to measure this distribution by means of resonance-enhanced multiphoton ionization (RMI), which promises to give a much better sensitivity than CARS. In addition, unlike CARS, RMI is also sensitive to atomic hydrogen, allowing a direct measurement of its density (in the electronic ground state) in a volume source. This new possibility is of great importance since hydrogen atoms are very effective in destroying negative ions through the associative detachment process, and in quenching vibrationally excited molecules.[5,6]

In this paper we will present results obtained with the RMI technique on molecules in the levels $v''=0$, 1, and 2 and on atomic hydrogen, all in their electronic ground state. Some of our results confirm facts already known from the CARS data,[8] others are an extension enabled by the fact that we can run our discharge at higher current and lower pressure while still observing a measurable signal.

II. EXPERIMENTAL SETUP

Details of the experimental setup and the RMI technique have been published elsewhere.[13] In short, the ion

source is a rectangular magnetic multipole bucket source with dimensions $14\times19\times14$ cm^3. Except for the front plate, all walls are equipped with permanent magnets generating a cusp field of ≈0.07 T on the inside. The front plate is electrically insulated from the rest of the walls and is biased to a cathode potential. Three sets of two tungsten filaments each are mounted in the back plate. The source is operated up to 30 A, 200 V dc (dc is direct current). Working pressure in the source is between 0.2 and 5 Pa. The source is not equipped with a magnetic filter and, as a consequence, we investigate the properties of the discharge in the "driver region," i.e., the region in a tandem source where the vibrational excitation is assumed to occur.[4]

The actual analysis with the RMI technique takes place outside the discharge. Through an aperture in the front plate, which also serves as a pumping hole, a hot gas jet effuses into the main vacuum vessel. The pressure in this vessel, far from the aperture, is ≈700 times lower than in the discharge chamber. Light from a pulsed tunable dye laser is frequency doubled and subsequently focused at a point ≈7 mm in front of the aperture. Quantum-state-specific detection of particles effusing from the discharge is achieved by means of selective ionization using the RMI principle, after which the resulting ions are detected. By measuring the RMI signal as a function of wavelength, information is obtained about the population of the different quantum states that are ionized. All measurements presented in this paper where obtained using three photons to excite the molecule or atom to an intermediate state, after which the absorption of one additional photon causes ionization, a process abbreviated as $(3+1)$ RMI. Discrimination against unwanted ions (such as plasma ions) is achieved by the combination of a magnetic (≈1 T) and an electric field (≈1 MV/m) at the laser focus. For each laser shot both H^+ and $H_2{}^+$ ionization signals and the laser pulse energy (as registered by a photodiode) are measured. To reduce the influence of shot to shot variations in laser intensity on the ionization signals, the measured signals are averaged over 30 laser shots at each wavelength. After each scan, these averages are stored on tape for plotting and further analysis.

III. MEASURING PROCEDURES AND DATA HANDLING

In Fig. 1 we give a simplified potential-energy diagram of the hydrogen molecule, featuring all electronic states that are referred to in this paper. For measurements on molecules in the $X\,{}^1\Sigma_g^+(v''=0)$ state one of the vibronic levels of the $C\,{}^1\Pi_u$ state was used for the intermediate level. In principle the ${}^1\Pi_u\leftarrow{}^1\Sigma_g^+$ vibrational bands have seven rotational branches of which we are able to observe the P ($\Delta J=-1$), Q ($\Delta J=0$), and R ($\Delta J=+1$) branches. ΔJ is the change in rotational quantum number in the three-photon excitation step. An example of such a transition is indicated in Fig. 1. The arrows represent photons around ≈290 nm, which excite molecules in the $X\,{}^1\Sigma_g^+(v''=0)$ state via two so-called virtual states indicated by the horizontal dotted lines, to the

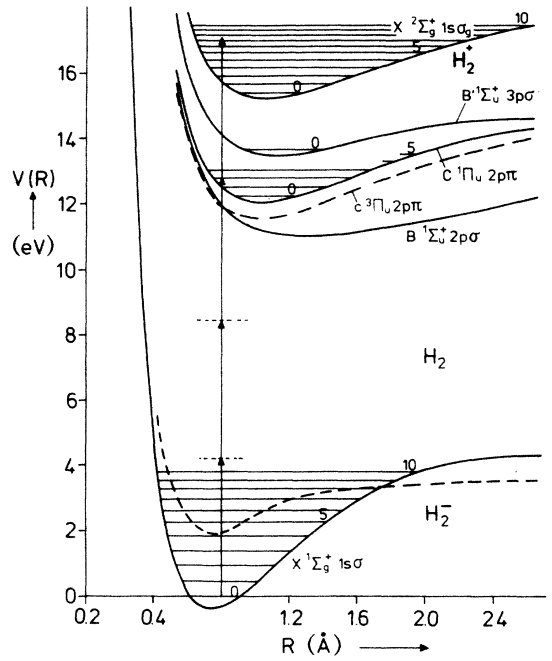

FIG. 1. Potential-energy diagram of the hydrogen molecule. Indicated is a three-photon transition from the $X\,{}^1\Sigma_g^+(v''=0)$ state to the $v'=2$ level of the $C\,{}^1\Pi_u$ state, proceeding via two virtual states represented by the dotted horizontal lines. The absorption of an additional photon causes ionization of the molecule.

$C\,{}^1\Pi_u(v'=2)$ state.[13] The absorption of one additional photon causes ionization. Because the Q branch is the strongest of the three branches observed, the Q lines were used to derive the relative populations of molecules in different rotational levels in the $v''=0$ level. As we reported previously,[14] a large share of the RMI signal, when using the $C\,{}^1\Pi_u\leftarrow X\,{}^1\Sigma_g^+$ bands, consists of H^+ ions. Therefore the relative populations determined from these measurements were deduced from the sum of H^+ and $H_2{}^+$ signals.

For measurements on molecules in the $X\,{}^1\Sigma_g^+(v''=1$ and 2) state, the $B'\,{}^1\Sigma_u^+(v'=0)$ level (see Fig. 1) was used for the intermediate level. The ${}^1\Sigma_u^+\leftarrow{}^1\Sigma_g^+$ vibrational bands have four rotational branches, of which we observe the P and R branches. This time we choose the R branch for deriving relative populations; again because these are the strongest lines, making it possible to observe the largest number of rotational levels. Unfortunately, the $R(0)$ and $R(1)$ peaks overlap for these bands and, therefore, we construct the intensity at the $R(1)$ peak from the measured intensities of the $P(1)$, $P(3)$, and $R(3)$ peaks. The relative intensity for the $P(1)$ and $P(3)$ peaks also gives the relative intensity for the $R(1)$ and $R(3)$ peaks. Multiplication of this ratio with the measured intensity of the $R(3)$ peak then gives the constructed intensity of the $R(1)$ peak. Measurements show that when using the $B'\,{}^1\Sigma_u^+(v'=0)$ level for the intermediate level, less than 20% of the ionization signal consists of H^+ ions. Moreover, the peaks for the

$v''=1$ and 2 measurements in the H^+ signal partially overlap with peaks resulting from other transitions, like those proceeding via $C\,^1\Pi_u(v'\geq 3)$ or $B\,^1\Sigma_u^+(v'\geq 10)$. Therefore only the $H_2{}^+$ signals were used in these measurements.

The assignment of the peaks in the RMI spectra is performed using the energy levels for the $X\,^1\Sigma_g^+$, $C\,^1\Pi_u$, and $B\,^1\Sigma_u^+$ states given by Dabrowski[15] and those for the $B'\,^1\Sigma_u^+$ state from Namioka.[16] From these energy levels and the above-mentioned selection rules, the value for each three-photon transition wavelength can be calculated.

The intensity of each transition $[S(i)]$ is determined from the spectra by summing the ionization signals, corrected for the background, within a wavelength interval associated with the corresponding peak. The width and position of the interval and the magnitude of the background is determined from the spectra "by the eye."

Because of the nonlinearity of the RMI process, the resulting ionization signals (S) depend in a nonlinear fashion on the laser intensity (I), i.e., $S=\sigma_N I^N$, where σ_N is the generalized cross section for the multiphoton ionization process and N is the coefficient of nonlinearity. Therefore if one wants to correct the measured spectra for variations in laser intensity, the spatial intensity distribution in the laser focus should be measured at each wavelength. With this distribution it is then possible to correct the ionization signal, as was demonstrated for nonresonant four-photon ionization of Cs atoms at 1.06 μm.[17] Because of the complexity of such a measurement and the time it takes to perform the required calculations in the correction procedure, we decided to correct the ionization signals just for variations in laser-pulse energy. By doing so, we, in fact, assume that the intensity in every point of the laser focus scales with the laser-pulse energy E and that during a wavelength scan this scaling remains the same. For scans, for instance, over the lines of a rotational branch in which the laser-pulse energy does not vary too dramatically (i.e., not more than $\approx 10\%$), we consider this assumption to be valid. The correction procedure is now the following: the mean pulse energy (E_m) within that particular scan and the mean pulse energy $[E_m(i)]$, within the wavelength interval corresponding to the ith peak, is determined from the averaged photodiode signals at each wavelength; the corrected intensity $[A(i)]$ for this peak is then obtained from the relation

$$A(i)=S(i)\left[\frac{E_m}{E_m(i)}\right]^N . \tag{1}$$

In general, it is reasonable to assume that for an RMI process, the step in which the largest number of photons is involved is rate limiting, and that the order of nonlinearity of the total process is equal to this number of photons. Consequently we use $N=3$ in Eq. (1). The validity of this assumption has been demonstrated, for instance, for (3 + 1) RMI of atomic hydrogen at ≈ 307.6 nm (Ref. 18) and ≈ 365 nm,[19] and for (3 + 2) RMI of Xe at ≈ 440.5 nm.[20]

The relative intensities within one rotational branch do not directly give the relative populations of the different J'' levels. In principle one should correct for the rotational line strengths, but these are not known to us for the three-photon excitation step and, therefore, we have taken them equal. This is a general problem in experiments where corrections should be made for multiphoton transition probabilities.[21] Consequently we take the relative intensities within the Q branch for the $v''=0$ measurements and within the R branch for the $v''=1$ and 2 measurements to be equal to the relative populations of the J'' levels within each vibrational level.

IV. ROTATIONAL DISTRIBUTIONS FOR $X\,^1\Sigma_g^+(v''=0, 1, \text{and } 2)$

A. Measurements

In Fig. 2 we present (3 + 1) RMI spectra appropriate to the ionization of molecules in the $X\,^1\Sigma_g^+(v''=0,$ 1, and 2) states as was discussed in Sec. III. Discharge parameters during the recording of these spectra are the

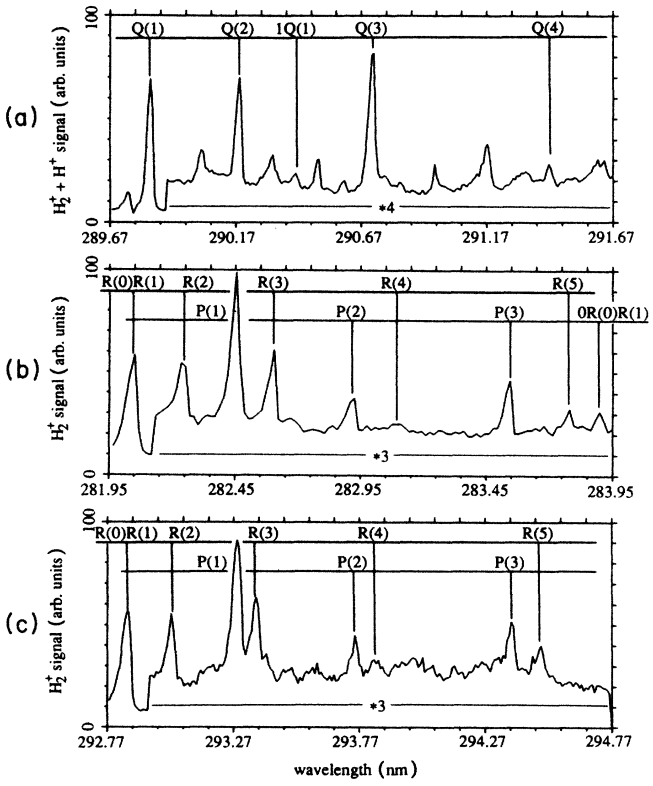

FIG. 2. (3+1) RMI spectra for $X\,^1\Sigma_g^+(v''=0,$ 1, and 2) molecules. The marked peaks in (a) originate from the $C\,^1\Pi_u(v'=2)\leftarrow X\,^1\Sigma_g^+(v''=0)$ transition, except for the peak marked $1Q(1)$ which is due to the $C\,^1\Pi_u(v'=4)\leftarrow X\,^1\Sigma_g^+(v''=1)$ transition. The marked peaks in (b) and (c) result from the $B'\,^1\Sigma_u^+(v'=0)\leftarrow X\,^1\Sigma_g^+(v'')$ transition with $v''=1$ and 2, respectively, except for the peak marked $0R(0)R(1)$ in (b), which originates from the $C\,^1\Pi_u(v'=3)\leftarrow X\,^1\Sigma_g^+(v''=0)$ transition. Note the indicated change in scale in each spectrum. Discharge parameters for these measurements are $I_d=10$ A, $P_d=1.2$ Pa, and $V_d=100$ V.

following: current $I_d = 10$ A, voltage $V_d = 100$ V, and pressure $P_d = 1.2$ Pa.

Figure 2(a) gives the result for the $C\,^1\Pi_u(v'=2) \leftarrow X\,^1\Sigma_g^+(v''=0)$ transition. Indicated are the members of the Q branch and, between parentheses, the rotational quantum number J'' of the level that is being ionized when the laser wavelength is at corresponding position. The peak marked $1Q(1)$ is the $Q(1)$ transition belonging to the $C\,^1\Pi_u(v'=4) \leftarrow X\,^1\Sigma_g^+(v''=1)$ transition, which will be discussed in Sec. V. Except for the peak at $\lambda \approx 290.97$ nm and the two small peaks immediately to the right of the peak marked $Q(3)$, all other peaks can be identified as three-photon excitations from the ground state to one of the vibronic levels of the $C\,^1\Pi_u$ or $B\,^1\Sigma_u^+$ states. The more or less wavelength-independent background signal in the scans in Fig. 2 is caused by one-photon ionization of metastable hydrogen molecules in the $c\,^3\Pi_u^-$ state[9] (see Fig. 1).

Figures 2(b) and 2(c) give the results for the $B'\,^1\Sigma_u^+(v'=0) \leftarrow X\,^1\Sigma_g^+(v'')$ transition with $v''=1$ and 2, respectively. Indicated are the members of the P and R branches, using the same notation as in Fig. 2(a). The peak marked $0R(0)R(1)$ in Fig. 2(b), which is the sum of the $R(0)$ and $R(1)$ peaks belonging to the $C\,^1\Pi_u(v'=3) \leftarrow X\,^1\Sigma_g^+(v''=0)$ transition, is the small part of the total ionization signal that appears in the H_2^+ channel. In the H^+ channel this peak is about 25 times as high. The fact that peaks related to different vibrational levels appear in the same wavelength interval, i.e., the $1Q(1)$ peak in Fig. 2(a) and the $0R(0)R(1)$ peak in Fig. 2(b), makes it possible to determine the vibrational temperature from these measurements (see Sec. V A).

From the spectra in Fig. 2 the relative populations of the J'' levels within each vibrational level were determined as described in Sec. III. Provided the occupation of the rotational levels is in thermal equilibrium, then the normalized distribution over the different rotational levels is given by

$$P_{J''} = \frac{(2J''+1)(2T+1)\exp[-E_r(J'')/kT_r]}{\sum_{J''}(2J''+1)(2T+1)\exp[-E_r(J'')/kT_r]}, \qquad (2)$$

in which $E_r(J'')$ is the rotational energy[15] of level J'', k is Boltzmann's constant, and T_r the rotational temperature. $(2J''+1)$ and $(2T+1)$ refer to the degeneracy of the rotational levels and nuclear-spin states, respectively. $T=0$ for even-J'' levels (parahydrogen) and $T=1$ for odd-J'' levels (orthohydrogen).

In order to see whether our measured populations are in line with Eq. (2), we plotted the quantity $\ln[(A(J'')/(2J''+1)(2T+1)]$ as a function of E_r/k for each of the measurements in Fig. 2. The results of these "Boltzmann plots" are shown in Fig. 3. If Eq. (2) were the correct distribution, the data points in each set should fall on a straight line with a slope equal to $-1/T_r$. The straight lines in Fig. 3 have been fitted to the data for $J''=1$, 2, and 3 using the least-squares criterion. The corresponding rotational temperatures are 390, 400, and 410 K for molecules with $v''=0$, 1, and 2, respectively. The uncertainty in these temperatures, es-

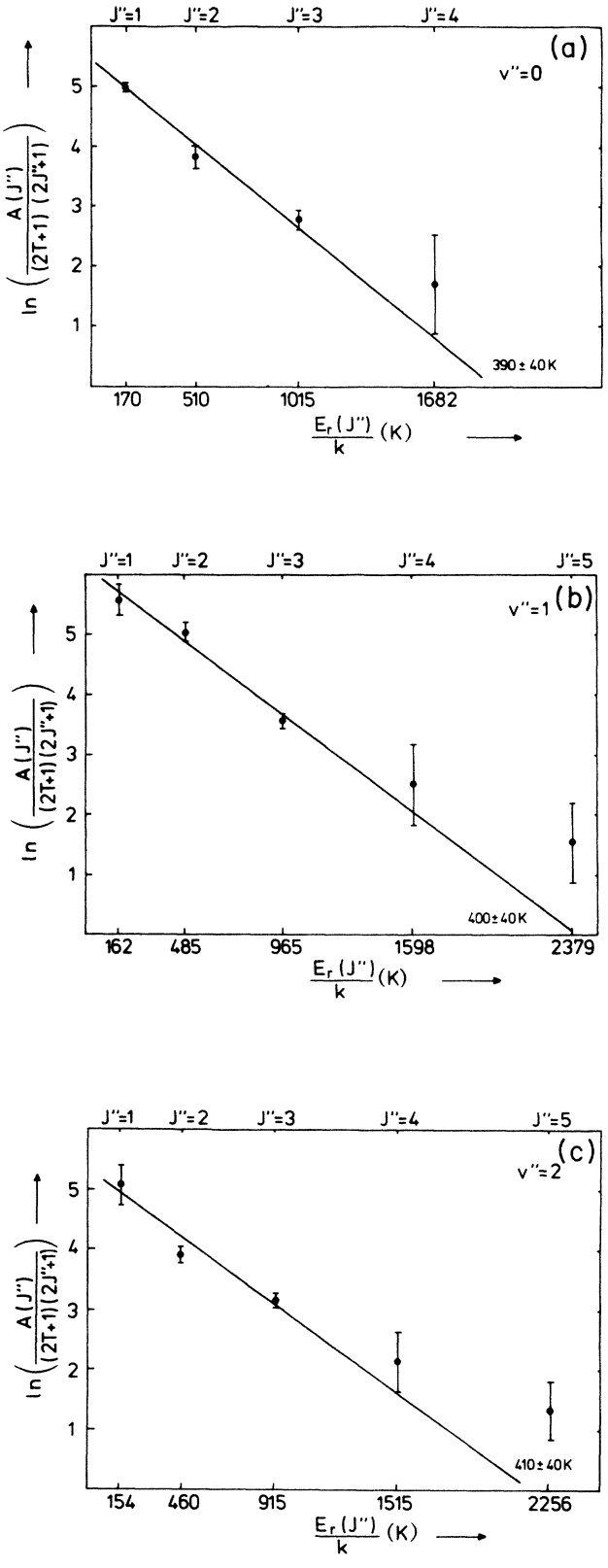

FIG. 3. Boltzmann plots for the corresponding measurements in Fig. 2. The straight lines were fitted to the data points for $J''=1$, 2, and 3, and their slopes correspond to a rotational temperature of $T_r = 390$, 400, and 410 K for $X\,^1\Sigma_g^+$ molecules in $v''=0$, 1, and 2, respectively.

timated from the error bars in the individual data points, is $\approx 10\%$. It is arguable whether the $J''=4$ populations are in equilibrium with the lower J'' levels, since the corresponding error bars still touch the straight line. However, it turns out that for almost all the measurements we have done on the rotational distributions with the discharge on, the data point for $J''=4$ is above the straight line calculated from the $J''=1$, 2, and 3 levels. For the $J''=5$ level there is no doubt that it is more populated than would be expected for the Boltzmann equilibrium at a temperature calculated from the lower levels. Similar deviations from the Boltzmann equilibrium have been found by Pealat *et al.*[8] as well. In order to quantify these results we calculated the overpopulation $O(J'')$ of the $J''=4$ and 5 levels, which we define as the ratio of the measured population to the population calculated from Eq. (2), fitted to the data points at $J''=1$, 2, and 3. In a Boltzmann plot this corresponds to the vertical distance between the data points and the straight line. Due to the uncertainty in T_r ($\approx 10\%$) and in the signals for $J''=4$ and 5, we obtain relatively large uncertainties in the calculated overpopulations. The results for T_r and $O(J'')$ for $v''=0$, 1, and 2 at various discharge currents are summarized in Table I. In addition, we measured T_r for $v''=0$ while varying V_d from 75 to 150 V and P_d from 0.3 to 1.7 Pa at constant I_d. Within the mentioned uncertainty no change in T_r was observed. Note that the values quoted for T_r are lower than those stated previously[9] due to the fact that T_r is determined from the signals at $J''=1$, 2, and 3 only, while for the previous values we used all measured levels.

An unexpected result is that when the discharge power supply is turned off, leaving the filament current and the gas flow running, scans like those in Fig. 2 still show the presence of vibrationally excited molecules in the discharge chamber, though at a much lower density.[22] At a filament current setting equal to the one used for a measurement at $I_d=30$ A we obtain $T_r\approx 350$ K for $v''=0$, and $T_r\approx 400$ K for $v''=1$ and 2 molecules.

At present we can only test the validity of our measuring procedures and analysis for molecules in the $X\,^1\Sigma_g^+(v''=0)$ state, when the discharge is turned off, giving hydrogen molecules in thermal equilibrium with the water-cooled discharge chamber wall (≈ 288 K).

TABLE I. Rotational temperatures (in K, $\pm 10\%$) and overpopulations (see the text for definition) for $X\,^1\Sigma_g^+(v''=0,1,2)$ molecules at difference discharge currents. Other discharge parameters are $V_d=100$ V and $P_d=1.2$ Pa.

State	I_d (A)	10	20	30
$v''=0$	T_r	370	420	430
	$O(4)$	2.0±0.4	1.9±0.4	1.8±0.4
$v''=1$	T_r	390	510	520
	$O(4)$	1.4±0.7	1.2±1	1.9±0.6
	$O(5)$	4.8±1.3	3.9±1.8	4.0±1.4
$v''=2$	T_r	390	450	520
	$O(4)$	2.1±0.5	2.8±0.5	1.5±1
	$O(5)$	5.2±1.5	5.9±2	5.3±2

From a measurement like the one in Fig. 2(a) we find under these conditions $T_r=280\pm 15$ K and $O(4)=1.1\pm 0.3$. This result confirms the reliability of our approach for the rotational distribution of $v''=0$ molecules. Since we do not have a calibrated source for the higher vibrational levels yet, we also use it as a proof for the correctness of the results concerning the other levels.

B. Discussion

Several processes come to mind which could be responsible for populating the higher rotational levels. We recall from the Introduction that the e-V process, proceeding via the H_2^- resonance $^2\Sigma_u^+$, is believed to play an important role in populating the lower vibrational levels in the discharge. However, with this process not only vibrational but also rotational excitation can be achieved.[23] Such in contrast to the E-V process, for which it is unlikely that a change in rotational quantum number will occur: Koot, van der Zande, and de Bruijn showed[24] that the rotational quantum number during ionization of H_2 molecules, in the $X\,^1\Sigma_g^+(v''=0)$ state, by 90-eV electrons remains unchanged, an aspect which we expect to be the same for excitations to the singlets of H_2. In addition, wall collisions, in which vibrational energy is converted into rotational and translational energy, provide an effective mechanism for populating high rotational levels,[25] just as the atom-exchange process.[26] Finally we observe that Kubiak, Sitz, and Zare[27] and Zacharias and David[28] find non-Boltzmann rotational distributions for hydrogen molecules produced via recombinative desorption of atomic hydrogen after permeation through Cu and Pd, respectively. Although the hydrogen atoms in our experiment are produced in the bulk of the discharge or on hot filament surfaces, recombination on the discharge chamber wall followed by desorption may contribute to the measured overpopulations. Especially the fact that vibrationally excited molecules are present in the discharge chamber with only filament current and gas flow running is an indication that this process takes place, seeing that we also detect hydrogen atoms under these conditions (see Sec. VI).

V. SCALING LAWS FOR $X\,^1\Sigma_g^+(v''=0,$ 1, and 2) MOLECULES

A. Measurements

Provided the rotational distribution within a vibrational level is known, it is possible to obtain a measure for the total population in that level from the intensity of the $Q(1)$ or $R(0)R(1)$ peak only. For this purpose we used the Boltzmann distribution given by Eq. (2), in which we evaluate the partition function in the denominator over the lowest six rotational levels using the measured value for T_r. In this way we neglect the measured deviations from the Boltzmann equilibrium for the $J''=4$ and 5 levels, and possibly of the higher J'' levels, which is justified by the observation that these levels contribute less than $\approx 5\%$ to the total population in each vibrational level.

Application of this procedure to the $Q(1)$ and $1Q(1)$ peaks in measurements like the ones in Fig. 2(a) yields a relation between the densities of molecules in the $v''=0$ and 1 states. In order to determine the ratio of their densities on an absolute scale, the obtained values have to be corrected for the change in ionization efficiency when employing the three-photon excitation step via different vibrational bands. To this end it seems reasonable to correct the ionization signals for the change in Franck-Condon factors for the $C\,^1\Pi_u^-(v'=2) \leftarrow X\,^1\Sigma_g^+(v''=0)$ and $C\,^1\Pi_u^-(v'=4) \leftarrow X\,^1\Sigma_g^+(v''=1)$ transitions: 0.1886 and 0.039 04, respectively.[29] In this way we obtain the absolute ratio (r) for the density of $v''=1$ over $v''=0$ molecules. Together with the energy difference between these two states, (E_{01}),[15] we derive a vibrational temperature (T_v) from the relation $T_v = E_{01}/(k \ln r)$. For lack of a calibration source, it is not yet possible to test the correctness of this procedure. The values of T_v thus obtained, as a function of discharge current, are given by the circles in Fig. 4. Note that these results are in agreement with those obtained by Pealat *et al.* ($T_v = 2390$ K at $I_d = 10$ A, $P_d = 5.5$ Pa).[8]

For measurements like those in Fig. 2(b) we obtain the $R(0)R(1)$ peak for $v''=0$ and 1 molecules within one scan, though via different electronic transitions (see Sec. IV A). This prevents us from calculating the absolute ratio of densities for molecules in $v''=0$ and 1 from these measurements, since the relative intensities of the two transitions involved are unknown. Therefore we use the measured ratio at 10 A, from measurements like those in Fig. 2(a), for calibration. These results are given by the triangles in Fig. 4 (circles and triangles coincide for $I_d = 5$ and 10 A). The advantage of this procedure lies in the fact that the peak from which the $X\,^1\Sigma_g^+(v''=1)$ population is derived is much larger in Fig. 2(b) than in 2(a). Thus we are able to measure with a larger sensitivity and now we can also determine the vibrational temperature with only the filament current and gas flow running. Again at a filament current setting equal to the one used for a measurement at $I_d = 30$ A we find in this way $T_v \approx 1400$ K.

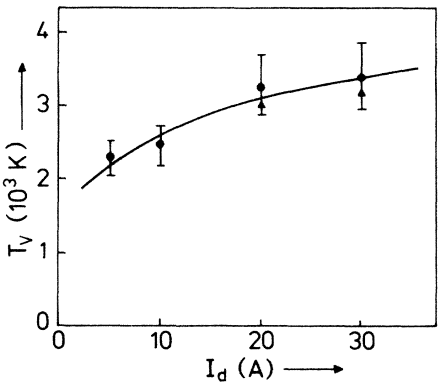

FIG. 4. Variation of the vibrational temperature, calculated from the $X\,^1\Sigma_g^+(v''=0$ and 1) populations, with discharge current, at $P_d = 1.2$ Pa and $V_d = 100$ V. Circles were derived from the peaks $Q(1)$ and $1Q(1)$, like those in Fig. 2(a), and triangles from the peaks $R(0)R(1)$ and $0R(0)R(1)$, like those in Fig. 2(b) (circles and triangles at $I_d = 5$ and 10 A coincide). For details on the correction procedure, necessary to account for the change in transition strength, see the text.

In order to obtain the variation of the density of molecules in a particular vibrational level with discharge parameters, we cannot measure complete spectra like in Fig. 2 for each parameter setting and then deduce, from the change of the peak intensities, the required information. Such a procedure calls for measuring times longer than the time over which the laser system is stable. This gives rise to changes in the relation between laser-pulse energy and light intensity in the laser focus, and it is no longer possible to relate signals obtained in one scan to those in another scan. Therefore we only measure the ionization signal at the top of the $Q(1)$ or $R(0)R(1)$ peak, i.e., at fixed wavelength, and immediately beside the peak, to obtain the background level. In this way, a measure for the intensity of the peak is obtained, which is converted to a measure for the total population, in the corresponding vibrational level, via the procedure described above.

The results of these measurements for $v''=0$, 1, and 2 are shown in Fig. 5 in which V_d was kept at a constant 100 V. We observe that the population of the $v''=0$ level declines with increasing discharge current I_d and is proportional to the source filling pressure P_d (with discharge on) up to ≈ 1 Pa. Above this pressure, the fraction with which the $v''=0$ density declines becomes smaller. In the pressure regime studied, the population of the $v''=1$ and 2 levels is proportional to P_d and independent of discharge current variations between 10 and 30 A. Therefore, in this regime the increase of T_v with I_d (see Fig. 4) is not caused by an increase of the $v''=1$ population but by a decrease of the $v''=0$ population.

B. Discussion of scaling laws for $X\,^1\Sigma_g^+(v''=0)$ molecules

The linear dependence of the $v''=0$ density on P_d without discharge is, of course, not surprising, nor is its decrease with increasing I_d, since they form the material for all discharge produced particles. Removal of a molecule from the $X\,^1\Sigma_g^+(v''=0)$ population, for instance by vibrational excitation or dissociation, requires a certain amount of energy. Therefore, the fraction of molecules removed from the $v''=0$ population cannot remain constant with increasing pressure, but has to decrease because the total amount of energy put into the discharge is limited. The onset of this effect is seen in our measurements on the $v''=0$ population at ≈ 1 Pa [see Fig. 5(a)]. In fact, for processes in which high-energy (>11 eV) electrons are required, it has been shown that this effect plays a role already above ≈ 0.4 Pa.[9]

In order to be more quantitative about the reduction of the $v''=0$ population, we note that the total particle flux through the aperture in the front plate has to remain constant since the source is operated at constant

gas flow. Because of the magnetic field of our detection system,[13] only neutral particles are able to pass the aperture, so that the flux consists of H_2 molecules in the electronic ground state $X\,^1\Sigma_g^+$, the metastable state $c\,^3\Pi_u^-$, and H atoms. Measurements have shown that the $c\,^3\Pi_u^-$ density is at most 10^{-4} times the gas density[9] and, therefore, we neglect them in the following analysis. Assuming that the velocity distribution of the $X\,^1\Sigma_g^+$ molecules and atoms can be characterized by a temperature, we obtain from the fact that the flux through the aperture remains constant

$$n_0\sqrt{T_0}=n\sqrt{T}+n_{\mathrm{H}}\sqrt{\tfrac{1}{2}T_{\mathrm{H}}}\ . \tag{3}$$

In Eq. (3) n_0, T_0, n, T, n_{H} and T_{H} are the total density

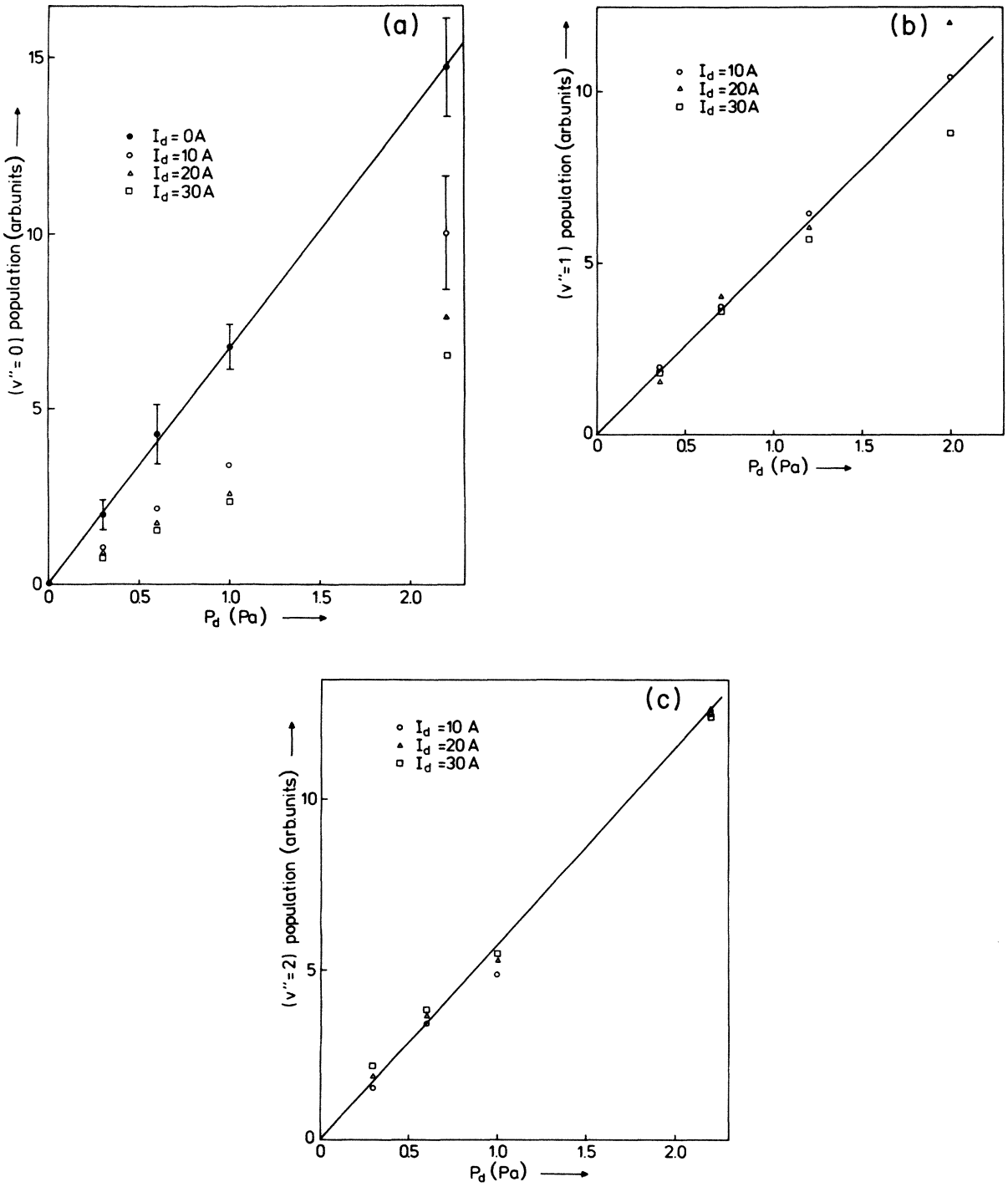

FIG. 5. Variation of the $X\,^1\Sigma_g^+(v''=0, 1, \text{and } 2)$ populations with discharge current and pressure. $V_d = 100$ V in these measurements.

and translational temperature of $X\,^1\Sigma_g^+$ molecules with the discharge off and on and the atomic density and temperature, respectively. The factor $\frac{1}{2}$ in front of T_H arises from the fact that it takes two H atoms to remove effectively one H_2 molecule from the discharge chamber and that an atom moves $\sqrt{2}$ times as fast as a molecule with the same amount of kinetic energy. Assuming the Boltzmann equilibrium between the lower rotational levels and translation, we use for T_0 and T the measured value of T_r for $v''=0$ molecules under various conditions. For T_H we do not have a measurement and, therefore, we use $T_H=4560$ K quoted by Pealat *et al.*[8] for $I_d=10$ A. By defining the relative residual molecular density as $\alpha_1=n/n_0$, the relative atomic density as $\alpha_H=n_H/n_0$, and substituting the values for T_0 (288 K) and T_H we derive from Eq. (3)

$$\alpha_H=0.021(17-\alpha_1\sqrt{T_r}) . \tag{4}$$

α_1 can be calculated from the data points in Fig. 5a, which give the decrease of molecules in $v''=0$ level, and the values for the vibrational temperature in Fig. 4, necessary to account for the molecules in the higher vibrational levels (at this point we assume Boltzmann equilibrium between the vibrational levels). T_r is obtained from Table I. The results for α_1 and α_H, expressed in %, are given in Table II. Barring the possible error in the value taken for T_H, the procedure followed results in an upper limit for α_H: the deficiency of H_2 molecules is entirely ascribed to atoms. Fair agreement is obtained with the value of the relative residual molecular density α_1 found by Pealat *et al.*[8] (71% at $I_d=10$ A, $P_d=5.5$ Pa), whereas the figures for the relative atomic density, α_H, both from Pealat *et al.*[8] (5%) and Nightingale *et al.*[10] (2–3) % at $I_d=25$ A, $P_d=0.4$ Pa) are obviously lower than our results. Note, however, that these results were derived from measured excited-state populations using high-resolution spectroscopy and laser-induced fluorescence, respectively. Due to the relatively large uncertainties in α_H, it is not possible to derive conclusions from Table II other than that the atomic density is of the order of 10–15 % of the molecular density without discharge. However, α_H shows a tendency to increase with discharge current while α_1 clearly decreases, resulting in a pronounced increase in the ratio of atomic to actual molecular density, which in our notation is equal to α_H/α_1.

C. Discussion of scaling laws for $X\,^1\Sigma_g^+(v''=1$ and 2) molecules

We start our analysis for the scaling laws of the density of molecules in $v''=1$ and 2 levels (n_1 and n_2, respectively) with the observation that the primary electrons are the source of all excitation. Knowledge of the dependence of their density n_p and energy-distribution function on discharge parameters is indispensable to gain insight into the processes taking place. Primary electrons are emitted from the filaments and obtain an initial velocity v_p. They are lost either to the walls of the discharge chamber, with a characteristic time τ_w, or by inelastic collisions with other particles. The characteristic time τ_{in} for the latter process may be expressed by

$$\tau_{in}\approx\frac{1}{n_g\langle\sigma_{in}v_p\rangle} , \tag{5}$$

with $\langle\sigma_{in}v_p\rangle$ the total reaction rate for inelastic collisions with unexcited gas molecules having a density n_g. By using Eq. (5) we neglect inelastic collisions of primary electrons with other than unexcited gas molecules. n_p may be calculated from the relation[30]

$$\frac{I_d}{eV}=n_p\left[\frac{1}{\tau_{in}}+\frac{1}{\tau_w}\right] , \tag{6}$$

in which e is the electron charge and V the volume of the discharge chamber. As soon as the gas density is so high that primary electron losses due to inelastic collisions dominate over those by wall losses, i.e., $n_g\langle\sigma_{in}v_p\rangle>1/\tau_w$, both density and energy-distribution function of the primary electrons are affected by n_g. From Eqs. (5) and (6) it is immediately clear that n_p becomes a decreasing function of n_g under these conditions. Following a similar calculation as was done by Bacal, Bruneteau, and Nachman,[7] it can be shown that this energy degradation effect becomes important in our source if $P_d>0.2$ Pa.

The equilibrium density n_j of any type of particle produced directly by primary electron excitation or ionization of unexcited molecules in the discharge is given by

$$n_j=n_g n_p\langle\sigma_j v_p\rangle\tau_j=\frac{n_g I_d\langle\sigma_j v_p\rangle\tau_j}{eV(n_g\langle\sigma_{in}v_p\rangle+1/\tau_w)} , \tag{7}$$

in which $\langle\sigma_j v_p\rangle$ is the reaction rate for the production of "j particles" and τ_j is their average lifetime in the discharge. In general τ_j is also a decreasing function of n_g and I_d. As a consequence, Eq. (7) predicts a proportional increase of n_j with n_g in the low-pressure regime where energy degradation can be neglected. For the higher pressures, n_j will become independent of n_g or even decrease with n_g, depending on the degree to which n_g affects τ_j. In addition, n_j is seen to be proportional to the discharge current I_d, as long as the lifetime τ_j is not affected by I_d. The variation of the density of metastable H_2 molecules, $c\,^3\Pi_u^-$, with n_g and I_d, for instance, can be understood on the basis of Eq. (7) if both energy

TABLE II. Relative residual molecular density (α_1) and relative atomic density (α_H) for different discharge currents and pressures. $V_d=100$ V in these measurements.

P_d (Pa)	I_d (A)	10	20	30
2.2	α_1	74±11	61±9	52±8
	α_H	6±6	9±6	13±5
1.0	α_1	55±8	44±7	41±6
	α_H	13±5	17±4	18±4
0.6	α_1	55±14	48±12	44±11
	α_H	13±7	15±7	16±6
0.3	α_1	57±14	55±14	48±12
	α_H	13±8	12±8	15±7

degradation and a reduction of their lifetime in the discharge τ_c with increasing n_g are incorporated.[9] Equation (7) also describes the density of particles produced via two-step processes in which $X\,^1\Sigma_g^+$ molecules are excited or ionized by primary electrons, after which these particles are converted into other particles as a result of radiative decay or wall collisions, but *not* by collisions with other particles present in the discharge chamber. Examples of such a two-step mechanism are the production of hydrogen atoms via triplet excitations and the production of vibrationally excited molecules by the *E-V* process or by Auger neutralization of H_2^+ ions. Not described by Eq. (7) are, for instance, the density of H^- ions or the density of vibrationally excited molecules produced by the *e-V* process. An extra complication lies in the fact that particles may be produced only partially by processes that can be described by Eq. (7), like vibrationally excited molecules that may very well be produced by both *E-V* and *e-V* processes, low-energy electrons, or atomic hydrogen.

The fact that n_1 and n_2 vary linearly with pressure implies that they are produced by means of a mechanism which, at least up to $P_d = 2.2$ Pa, does not suffer from energy degradation, and that the collisional deexcitation by other gas molecules still can be neglected at this pressure. From the observations that the cross sections for electron excitation to $c\,^3\Pi_u^-(v''=0)$ (Ref. 31) and to $X\,^1\Sigma_g^+(v''=1,2)$ via the *E-V* process[32] have comparable threshold energies (11–12 eV), and that for $c\,^3\Pi_u^-$ formation the influence of energy degradation has been demonstrated,[9] we conclude that the *E-V* process cannot be responsible for the production of $X\,^1\Sigma_g^+(v''=1,2)$ molecules in our discharge. The same reasoning also rules out formation of these molecules via Auger neutralization of H_2^+ ions at the discharge chamber walls. Although these conclusions were drawn earlier from model calculations,[5,6] ours is the first experimental evidence of their correctness. Production of $X\,^1\Sigma_g^+(v''=1,2)$ molecules via the *e-V* process is, as a consequence of its low-threshold energy, not in contradiction with our results, provided the plasma electron-energy distribution function around 1 eV is insensitive to P_d in the range studied, which seems plausible on the basis of calculations for electrons in a discharge similar to ours.[33]

Taking these observations into account, we write, analogous to Eq. (7), for the equilibrium density n_1 of molecules in the $X\,^1\Sigma_g^+(v''=1)$ state

$$n_1 \approx n_g n_e \langle \sigma_1 v_e \rangle \tau_1 \ . \tag{8}$$

In Eq. (8) n_e and v_e are the plasma electron density and velocity, respectively, $\langle \sigma_1 v_e \rangle$ is the reaction rate for production of $X\,^1\Sigma_g^+(v''=1)$ molecules from $X\,^1\Sigma_g^+(v''=0)$ by plasma electrons, and τ_l, which is a function of n_g and I_d, is the $X\,^1\Sigma_g^+(v''=1)$ lifetime in the discharge. The important difference between Eqs. (7) and (8) lies in the fact that in the latter the plasma electrons provide the source for the excitation, whereas in Eq. (7) the excitation comes directly from the primary electrons. In accordance with Eq. (7), the plasma electron density may be approximated by

$$n_e \approx n_g n_p \langle \sigma_i v_p \rangle \tau^- \ , \tag{9}$$

with $\langle \sigma_i v_p \rangle$ the reaction rate for ionization of $X\,^1\Sigma_g^+(v''=0)$ molecules by primary electrons and τ^- the plasma electron lifetime. For the $X\,^1\Sigma_g^+(v''=1)$ lifetime in the discharge we write

$$\tau_1 \approx \frac{1}{\nu_1/b_1 L + n_g \langle \sigma_g v_g \rangle + n_p \langle \sigma_p v_p \rangle + n_g n_p \sum_j \langle \sigma_j v_p \rangle \tau_j \langle \sigma_{d,j} v_j \rangle} \ , \tag{10}$$

in which the summation in the denominator covers all particles described by Eq. (7). In Eq. (10) v_1, v_g, and v_j denote the speed of $X\,^1\Sigma_g^+(v''=1)$ and $X\,^1\Sigma_g^+(v''=0)$ molecules and j particles, respectively. The reaction rates for destruction of $X\,^1\Sigma_g^+(v''=1)$ molecules by $X\,^1\Sigma_g^+(v''=0)$ molecules, primary electrons, and j particles are given by $\langle \sigma_g v_g \rangle$, $\langle \sigma_p v_p \rangle$, and $\langle \sigma_{d,j} v_j \rangle$, respectively; b_1 is the number of wall collisions it takes to deexcite $X\,^1\Sigma_g^+(v''=1)$ molecules and L is the average distance to the wall. The four terms in the denominator in Eq. (10) represent the losses of $X\,^1\Sigma_g^+(v''=1)$ molecules caused by collisions with the walls, $X\,^1\Sigma_g^+(v''=0)$ molecules, primary electrons, and j particles, respectively. Neglected are the losses caused by collisions with other discharge-produced particles, which is justified from the observation that their density is at least an order of magnitude lower than the $X\,^1\Sigma_g^+(v''=0)$ density.

Combination of Eqs. (8)–(10) leads to an expression for the equilibrium density n_1 of $X\,^1\Sigma_g^+(v''=1)$ molecules

$$n_1 \approx \frac{n_g^2 n_p \langle \sigma_i v_p \rangle \tau^- \langle \sigma_1 v_e \rangle}{\nu_1/b_1 L + n_g \langle \sigma_g v_g \rangle + n_p \langle \sigma_p v_p \rangle + n_g n_p \sum_j \langle \sigma_j v_p \rangle \tau_j \langle \sigma_{d,j} v_j \rangle} \ . \tag{11}$$

For $X\,^1\Sigma_g^+(v''=2)$ molecules similar formulas such as Eqs. (8), (10), and (11) hold.

Without performing sophisticated calculations combined with the knowledge of all relevant cross sections, it is impossible to draw *a priori* conclusions from Eq. (11). However, with our measurements in hand, it is possible to determine the dominant term in the denominator. For this purpose we write down Eq. (11) four

times, in each case assuming that one of the four terms in the denominator is dominant over the other three. In addition we make the first-order approximations that τ^-, $\langle \sigma_1 v_e \rangle$ and the ratios $\langle \sigma_i v_p \rangle / \langle \sigma_p v_p \rangle$ and $\langle \sigma_i v_p \rangle / \langle \sigma_j v_p \rangle$ are independent of n_g. Equations (5) and (6) are used to eliminate n_p and we obtain successively

$$n_1 \approx \frac{n_g^2 I_d \langle \sigma_i v_p \rangle c_1}{eV v_1 / b_1 L (n_g \langle \sigma_{\text{in}} v_p \rangle + 1/\tau_w)} , \tag{12a}$$

$$n_1 \approx \frac{n_g I_d \langle \sigma_i v_p \rangle c_1}{eV \langle \sigma_g v_g \rangle (n_g \langle \sigma_{\text{in}} v_p \rangle + 1/\tau_w)} , \tag{12b}$$

$$n_1 \approx n_g^2 c_1 c_2 , \tag{12c}$$

and

$$n_1 \approx \frac{n_g c_1}{\sum_j c_{3,j} \tau_j \langle \sigma_{d,j} v_j \rangle} , \tag{12d}$$

with c_1, c_2, and $c_{3,j}$ constants. Similar formulas apply to $X\,{}^1\Sigma_g^+(v''=2)$ molecules.

If the first term (wall losses) in the denominator in Eq. (11) were dominant, according to Eq. (12a) n_1 would vary linearly with n_g only if $n_g \langle \sigma_{\text{in}} v_p \rangle \gg 1/\tau_w$, which implies complete energy degradation. However, this seems unrealistic since n_e still increased with n_g in this pressure regime as was measured by others.[7] In addition, n_1 would vary linearly with I_d, which is clearly in contradiction with our measurements. It is seen that Eq. (12b) only predicts the linear increase of n_1 with n_g if there were no energy degradation at all, which is in contradiction with our own measurements on the $c\,{}^3\Pi_u^-$ density[9] and those by others.[7] In this case, too, we obtain the wrong linear increase of n_1 with I_d. The dominance of the third term could account for n_1 and n_2's independence of I_d. However, Eq. (12c) predicts a quadratic increase with n_g, which is again in contradiction with our measurements. Only if the last term is dominant we obtain complete agreement with the measured scaling laws, regardless of the extent to which the primary electrons are degraded in energy. The most prominent candidates in the denominator of Eq. (12d) which might be responsible for destruction of $X\,{}^1\Sigma_g^+(v''=1,2)$ molecules are H atoms, having a large deactivation coefficient for vibrational energy,[5,6] and plasma electrons, for which measurements in post discharges indicate that a coupling exists between their kinetic energy and the vibrational energy of H_2 molecules by superelastic collisions.[34]

VI. SCALING LAWS FOR ATOMIC HYDROGEN

A. Measurements

Measurements on scaling laws for atomic hydrogen were performed using a (3+1) RMI scheme at $\lambda \approx 364.4$ nm where three photons are resonant with the $1s$-$2p$ Lyman-α transition. Again we measure at a fixed wavelength at the top of and beside the peak in order to obtain a direct measure for the atomic ground-state population as a function of discharge parameters. The results, at $V_d = 100$ V, are given in Fig. 6. Plotting these data as a function of I_d, at constant P_d, indicates that the atomic density is proportional to I_d, with a start of saturation for the highest current used. Just as with vibrationally excited molecules, measurements also show the presence of atomic hydrogen with only the filament current and gas flow running. The atomic density, immediately after the discharge power supply was switched off, is proportional to n_g with a somewhat more gradual slope than the straight lines drawn in Fig. 6, indicating that the density of atomic hydrogen "not produced by the filaments" only shows a weak increase with n_g.

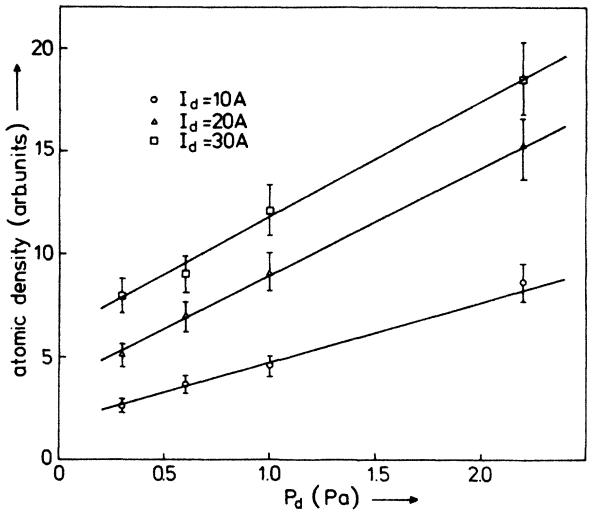

FIG. 6. Variation of the atomic density with discharge current and pressure. $V_d = 100$ V in these measurements.

B. Discussion

We ascribe the presence of H atoms without discharge current to thermal dissociation of H_2 molecules on the hot tungsten filament surfaces.[22] At an estimated temperature of the filaments of ≈ 2500 K and a pressure of ≈ 1 Pa, we calculate from the equilibrium constant K_p for the reaction $H_2 \rightleftharpoons 2H$ (Ref. 35) that the equilibrium degree of dissociation $n_H/(n_H + 2n_{H_2}) \approx 0.94$. However, due to the finite residence time of particles on the hot filament surface, it is doubtful whether equilibrium can be reached. Apparently the filament surface itself functions as a catalyst, making it possible that a measurable amount of H_2 molecules can be thermally dissociated during the residence time. Recombinative desorption of atomic hydrogen from the discharge walls may then contribute to the $X\,{}^1\Sigma_g^+(v''>0)$ population,[27,28] which we presume to be the mechanism responsible for the presence of vibrationally excited molecules with only gas flow and filament current on (see Sec. IV).

According to Eq. (7), production of atomic hydrogen in the discharge by primary electron excitation of $X\,{}^1\Sigma_g^+(v''=0)$ molecules followed by dissociation, is in agreement with the measured scaling laws, provided that the atomic lifetime in the discharge τ_H is independent of n_g and I_d (at least up to 20 A), i.e., destruction of atomic

hydrogen is dominated by wall collisions in this regime. If such were not the case, the density of atomic hydrogen in the discharge, corrected for the amount produced on the filaments, would show a decrease as a function of pressure, just like the density of $c\ ^3\Pi_u^-$ molecules.[9] The start of saturation of the atomic density above $I_d = 20$ A may be an indication of the existence of an additional mechanism, for which the corresponding atomic destruction rate becomes comparable to the losses suffered by wall collisions.

We note that the small increase of α_H with I_d at constant P_d (see Table II) seems to be inconsistent with the measured proportionality of the atomic density to I_d (see Fig. 6). This would imply that we cannot ascribe the measured deficiency of H_2 molecules entirely to atomic hydrogen, i.e., our analysis that leads to Eqs. (3) and (4) is partially incorrect. One of the major assumptions leading to Eq. (4) is the fact that the velocity distribution of the hydrogen molecules (and atoms) can be characterized by a temperature, which, in addition, is taken to be equal to the measured rotational temperature. However, Otorbaev *et al.*[36] reported that the molecular velocity distribution in a similar plasma is not Maxwellian but contains a high velocity tail. If this was the case in our discharge as well, the actual molecular deficiency would be less and consequently the calculated atomic density would also be lower. The latter aspect would also enhance the consensus with measurements by others[8,10] concerning the atomic level population.

VII. SUMMARY

In the pressure regime from 0.3 to 2.2 Pa, the density of H_2 molecules in the $X\ ^1\Sigma_g^+(v''=1$ and 2) state is measured to be proportional to the gas density and independent of discharge current variations between 10 and 30 A. Analysis of these results, using simple rate equations and taking into account the effect of energy degradation of the primary electrons, leads to the conclusion that these molecules are produced via low-energy-electron collisions with $X\ ^1\Sigma_g^+$ molecules [$(e\text{-}V)$ process] and that their destruction is dominated by collisions with other discharge produced particles, most probably H atoms and/or thermal electrons.

In the same regime, the ground-state atomic hydrogen density is found to be only weakly dependent on the gas density and proportional to the discharge current. These observations are explained with formation of atomic hydrogen by primary electron excitations of $X\ ^1\Sigma_g^+$ molecules, followed by dissociation, and destruction dominated by wall collisions.

If the heating current through the filaments and the gas flow is turned on, but the discharge power supply left off, both atoms and vibrationally excited molecules are still detected. For these phenomena we only give a tentative explanation, which has to be verified by additional measurements.

ACKNOWLEDGMENTS

This work is part of the research program of the association agreement of EURATOM and the Stichting voor Fundamenteel Onderzoek der Materie (FOM) with financial support from the Nederlandse Organisatie voor Zuiver Wetenschappelijk Onderzoek (ZWO) and EURATOM.

[1]Wulf B. Kunkel, IEEE Trans. Nucl. Sci. **26**, 4166 (1979); A. J. T. Holmes, L. M. Lea, A. F. Newman, and M. P. S. Nightingale, Rev. Sci. Instrum. **58**, 223 (1987).

[2]*Proceedings of the Second European Conference on the Production and Application of Light Negative Ions, Palaiseau, France, 1986,* edited by M. Bacal and C. Mouttet (Ecole Polytechnique, Palaiseau, 1986).

[3]*Proceedings of the Fourth International Symposium on the Production and Neutralization of Negative Hydrogen Ions and Beams, Upton, New York, 1986,* edited by J. Alessi (AIP, New York, 1987).

[4]J. R. Hiskes, Comments At. Mol. Phys. **19**, 59 (1987).

[5]C. Gorse, M. Capitelli, J. Bretagne, and M. Bacal, Chem. Phys. **93**, 1 (1985).

[6]J. R. Hiskes, A. M. Karo, M. Bacal, A. M. Bruneteau, and W. G. Graham, J. Appl. Phys. **53**, 3469 (1982); J. R. Hiskes, A. M. Karo, and P. A. Willmann, J. Vac. Sci. Technol. A **3**, 1229 (1985); J. Appl. Phys. **58**, 1759 (1985).

[7]M. Bacal, A. M. Bruneteau, and M. Nachman, J. Appl. Phys. **55**, 15 (1984).

[8]M. Pealat, J-P. E. Taran, M. Bacal, and F. Hillion, J. Chem. Phys. **82**, 4943 (1985).

[9]J. H. M. Bonnie, P. J. Eenshuistra, and H. J. Hopman, Phys. Rev. Lett. **57**, 3265 (1986).

[10]M. P. S. Nightingale, A. J. T. Holmes, M. J. Forrest, and D. D. Burgess, J. Phys. D **19**, 1707 (1986).

[11]M. Allan and S. F. Wong, Phys. Rev. Lett. **41**, 1791 (1978).

[12]J. M. Wadehra and J. N. Bardsley, Phys. Rev. Lett. **41**, 1795 (1978); Phys. Rev. A **20**, 1398 (1979).

[13]J. H. M. Bonnie, E. H. A. Granneman, and H. J. Hopman, Rev. Sci. Instrum. **58**, 1353 (1987).

[14]J. H. M. Bonnie, P. J. Eenshuistra, J. Los, and H. J. Hopman, Chem. Phys. Lett. **125**, 27 (1986); J. H. M. Bonnie, J. W. J. Verschuur, H. J. Hopman, and H. B. van Linden van den Heuvell, *ibid.* **130**, 43 (1986).

[15]I. Dabrowski, Can. J. Phys. **62**, 1639 (1984).

[16]T. Namioka, J. Chem. Phys. **41**, 2141 (1964).

[17]L. A. Lompre, G. Mainfray, and J. Thebault, Rev. Phys. Appl. **17**, 21 (1982).

[18]H. G. Muller, H. B. van Linden van den Heuvell, and M. J. van der Wiel, Phys. Rev. A **34**, 236 (1986).

[19]D. E. Kelleher, M. Ligare, and L. R. Brewer, Phys. Rev. A **31**, 2747 (1985).

[20]P. Kruit, J. Kimman, H. G. Muller, and M. J. van der Wiel, J. Phys. B **16**, 937 (1983).

[21]L. F. DiMauro, R. A. Gottscho, and T. A. Miller, J. Appl. Phys. **56**, 2007 (1984); E. E. Marinero, C. T. Rettner, and R. N. Zare, Phys. Rev. Lett. **48**, 1323 (1982).

[22]P. J. Eenshuistra, J. H. M. Bonnie, and H. J. Hopman (unpublished).
[23]G. J. Schultz, Rev. Mod. Phys. **45**, 423 (1973).
[24]W. Koot, W. J. van der Zande, and D. P. de Bruijn, Chem. Phys. **115**, 297 (1987).
[25]A. M. Karo, J. R. Hiskes, and R. J. Hardy, J. Vac. Sci. Technol. **A3**, 1222 (1985).
[26]E. E. Marinero, C. T. Rettner, and R. N. Zare, J. Chem. Phys. **80**, 4142 (1984).
[27]G. D. Kubiak, G. O. Sitz, and R. N. Zare, J. Chem. Phys. **83**, 2538 (1985).
[28]H. Zacharias and R. David, Chem. Phys. Lett. **115**, 205 (1985).
[29]D. C. Cartwright and S. Drapatz, Astron. Astrophys. **4**, 443 (1970).
[30]K. N. Leung, R. D. Collier, L. B. Marshall, T. N. Gallaher, W. H. Ingham, R. E. Kribel, and G. R. Taylor, Rev. Sci. Instrum. **49**, 321 (1978).
[31]N. J. Mason and W. R. Newell, J. Phys. B **19**, L587 (1986).
[32]J. R. Hiskes, J. Appl. Phys. **51**, 4592 (1980).
[33]J. Bretagne, C. Gorse, M. Capitelli, and M. Bacal, in Ref. 2, pp. 55–60.
[34]M. B. Hopkins and W. G. Graham, in Ref. 3, p. 166.
[35]*The Perfect Gas,* Vol. 5 of *The International Encyclopedia of Physical Chemistry and Chemical Physics,* edited by J. S. Rowlinson (Pergamon, New York, 1963), p. 85.
[36]D. K. Otorbaev, V. N. Ochkin, N. G. Preobrazhenskii, S. Yu. Savinov, A. I. Sedelnikov, and N. N. Sobolev, Zh. Eksp. Teor, Fiz. **81**, 1626 (1981) [Sov. Phys.—JETP **54**, 865 (1981)].